Iterative Design of Antenna Structures

R. Levy
DSIF Engineering Section

A new procedure is described for the design of antenna reflector structures for improved performance when subjected to the operational gravity loading. The design objective is to reduce the difference in pathlength of the RF energy beam that is reflected from the deformed surface with respect to the pathlength of the beam from a perfect paraboloidal surface. A virtual work formulation is used to state this objective in terms of the bar areas that compose the structure, which become the design variables. A special application of the Lagrange multiplier technique defines preferential redistributions of the design variables to improve performance. Improvements are developed subject to a primary constraint on total structure weight and additional practical side constraints. Design examples show efficient and effective applications of the described procedure.

I. Introduction

This article describes the mathematical procedure, implementation, and results of a computer program for parabolic antenna structure design to improve performance for gravity loading.

Performance of an initial, or preliminary, design can be improved by controlling the surface distortions caused by environmental loading. This loading is either random, such as results from wind and temperature, or deterministic from the effect of gravity. The gravity load results from the weight and the change in direction of the weight vector relative to the structure with changes in antenna elevation attitude. Within these two classifications, only the gravity loading is both omnipresent and predictable, and it also tends to be the most significant with respect to performance. Therefore, design of the structure to control gravity loading distortions is a logical and feasible approach towards performance enhancement.

II. Related Background Research

In the last decade there has been substantial effort and literature describing diverse approaches in the field of

structural design. This work typically is classified within the technology of structural optimization. Much of this background research, however, has only indirect bearing on reflector structure design or upon the procedures to be described here.

Structural optimization has most frequently considered design for minimum structural weight (Ref. 1), subject to various primary behavioral constraints (such as stress, buckling, displacement) and side constraints (such as fabrication requirements). Here we will consider the reflector structure problem as a design for improved performance, rather than minimum weight. The structure weight will be the primary constraint and the behavioral constraints will be side constraints.

A special requirement, which is not usually considered for static loading, is that the loading should not be treated as invariant. This is necessary because the weight of the structural components, which is significant, is redistributed during design. Furthermore, instead of examining a limited number of design loading cases, reflector design is concerned with an infinite set of loadings in which the orientation of the gravity loading vector changes over a continuous range of antenna elevation attitudes.

An important background idea relating to reflector design is Von Hoerner's concept of homologous design (Ref. 2). In this, the design is established to make the deformations under loading conform to a parabolic surface. A homologous design, however, is not always achievable. In our approach, although we recognize and employ related concepts, no directed attempt is made toward achieving the perfectly homologous design.

Von Hoerner also supplies one of the relatively few procedures for static design which include variability of loading. This effect has also been considered in Ref. 3 with design for a minimum-weight objective in the presence of deflection constraints. Variability of loading is inherent in the relatively virgin field of design for dynamic constraints, and prevalent approaches are surveyed in Ref. 4.

Other design optimization techniques that are the most closely related to the procedures that will be used here are described in Refs. 5, 6, and 7. These procedures adopt optimality criteria for stress as a constraint and incorporate virtual work formulations to express displacements as other constraints. In particular, Gellatly and Berke (Ref. 6) show that the Lagrange multiplier technique is effective in developing design improvements for practical structures with realistic numbers of variables and degrees of freedom. Kicher (Ref. 8) provides a comprehensive description of the application of the Lagrange multiplier within structural design.

III. Present Approach

The approach is to develop a mathematical definition of the design objective by means of a virtual work formulation. The objective function is then used with a special application of the Lagrange multiplier technique to develop an improved design. Since the design technique employed entails approximations, it is necessary to proceed iteratively towards the final design. The cyclic steps repeated during the iterations are analysis of the current design (mathematically "exact") and development of a preferential design (mathematically "inexact") from the analysis. Most of the prevalent structural design approaches are also iterative in this same way.

Mathematical derivation of the objective is founded upon the recently developed "rigging angle" concept (Refs. 9 and 10). This concept implies that the gravity loading at the so-called "rigging angle" attitude is compensated by adjustment of surface panels and the loading at other attitudes is effectively the net loading in moving away from the rigging attitude.

IV. Problem Formulation

A convenient measure of performance for design is the root mean square of half the difference in pathlength of the RF energy beam in traveling from a deformed reflector surface to the focal point compared with the pathlength from a surface that is a perfect paraboloid. The reflector surface of interest is equivalent to an infinite set of points for which pathlength differences exist; in practice the surface is replaced by a finite set of "target" points which are taken to be a representative sample of the entire set.

Accordingly, minimization or reduction of the mathematical expression for this half pathlength difference for gravity loading is taken to be the design objective function. The design variables are the cross-sectional areas of the individual bar members that compose the typical space–truss type of reflector structure. The primary constraint is a prespecified invariant total structure weight. Side constraints of minimum member sizes can be specified to preclude overstress and buckling. Additional constraints can be imposed to restrict the numbers of different member sizes. This last constraint is for fabrication economy and simplification. It is enforced by assigning par-

ticular members to groups that are required to have common sizes.

The foregoing definitions of objective function, design variables, and constraints categorize this as a problem of optimum design. Effectively, the problem is to redistribute a fixed amount of structural material to obtain an admissible design with improved performance. Here, the word "improved" is a realistic replacement for the word "optimum." The replacement is made because the (global) optimum is often undefinable, unachievable by direct procedures, or does not justify the undue effort that could be spent in the achievement.

This problem statement is essentially the same as for the Parabolic Antenna Reflector Design System (PARADES) program (Ref. 11). Here, however, we will describe a parallel in-house JPL effort that uses a different mathematical attack and a computer program that, although decidedly effective, is considerably less complex and, consequently, operates within a narrower scope.

V. Mathematics of Design Procedure

The improved design is developed by employing the virtual work principle to express an objective function stated in terms of the design variables and then using the Lagrange multiplier method to find new values of the design variables that improve the objective. Before doing this, it is helpful to describe the associated reflector surface geometry.

A. Reflector Geometry

The coordinate system used is shown in Fig. 1. The figure shows an antenna at a particular elevation attitude angle α. An X–Y–Z Cartesian coordinate system with origin at the paraboloidal vertex is defined. The Z-axis is the focal axis and the Y–Z plane is usually a plane of symmetry. The gravity loading is shown resolved into components parallel to the Y and Z axes.

The pathlength geometry relationship is shown diagrammatically in Fig. 2. Solid line V–G–C represents the original surface and the broken line represents the deflected surface. Target point G on the original surface is shown as deflected to point D. An incident ray parallel to the focal axis is shown crossing the aperture plane at A and is reflected at D to the focal point. With respect to the original surface, an alternative ray is shown to cross the aperture plane at B and then to be reflected at C to the focal point along the path C–D. Consequently, from the figure, it can be seen that the pathlength difference for these two rays is the sum of the distances from E to C and from C to D. The component of the deflection normal to the surface is indicated by the dimension dn.

B. Virtual Work Principle

For practical purposes, and within minor approximation, the reflector structure can be considered as a framework of m one-dimensional bars, each of which is completely characterized by its area A, length L, elastic modulus E, and its density. For simplicity, and consistent with practical applications, assume that the modulus and density are the same for all bars. Let the structure be subjected to a real external loading vector $\{P\}$ and let $\{S\}$ be the associated vector of internal forces (stress resultants). In addition, define a dummy single load D of unit magnitude applied in a specified direction at one particular node of the structure and let $\{U\}$ be the associated internal force vector. Then, from the principle of virtual work,

$$1 \cdot \delta = \sum_{i=1}^{m} [(S_i L_i)/(A_i E)] \cdot U_i \qquad (1)$$

where δ is the displacement of the structure at this node in the direction of D caused by the real load. In Eq. (1), the term on the left is the virtual external work of the unit load moving through the real displacement δ. The summation on the right is the internal virtual work expressed as the product of the real extension of each bar and the internal force caused by D. For a linearly elastic structure, Eq. (1) can be extended by superposition to represent the sums of the squares of the half pathlength difference of a set of surface target points from a perfect paraboloid. To do this, note that the half pathlength difference of a typical target point can be expressed as (Ref. 12)

$$\rho = \gamma_z \cdot dn \qquad (2)$$

where γ_z is the direction cosine of the surface normal with respect to the reflector focal axis and dn is the component of distortion normal to the surface. Then, in Eq. (1), apply the unit load normal to the surface, and the summation on the right will give δ on the left equal to dn. Furthermore, replace the unit dummy load by a load normal to the surface of magnitude

$$D = \gamma_z^2 \cdot dn \qquad (3)$$

Then it follows that Eq. (1) will give the square of the half pathlength difference at this target point as follows:

$$\rho^2 = \gamma_z^2 \cdot dn^2 = \sum_{i=1}^{m} (S_i U_i L_i)/(A_i E) \qquad (4)$$

where each U_i is the internal force of the single dummy load $\gamma_z^2\, dn$. Finally, apply a dummy loading vector $\{D\}$ that contains one load for each of n surface target points, each load applied normal to the local surface, with magnitude computed according to Eq. (3). Then by superposition it follows that the sums of squares of half pathlength deviations SS are given by

$$SS = \{\rho\}^t \{\rho\} = \sum_{i=1}^{m} (S_i U_i L_i)/(A_i E) \tag{5}$$

in which each U_i is the internal force for loading vector {D}. Finally, the rms half pathlength difference for the real loading is

$$\text{rms} = (SS/n)^{1/2} \tag{6}$$

Consequently, a reduction of the objective function (Eq. 5) results in reduction of the rms half pathlength differences (Eq. 6).

C. Objective Function

We will give a brief summary of pathlength difference and rigging angle relationships derived in Refs. 9 and 10. It was shown there for a linearly elastic structure that the displacements of the target set of points for two particular loading conditions provide sufficient information for the computation of the sums of squares of the half pathlength differences at any elevation attitude of the antenna. With reference to Fig. 1, the two required loading vectors, derived from the weight of all of the structural members plus supported non-structural components, are:

$\{P_y\}$ = loading vector for weight loading applied parallel to the reflector Y-axis.

$\{P_z\}$ = loading vector for weight loading applied parallel to the reflector Z-axis.

and let $\{u_y\}, \{u_z\}$ be the associated displacement vectors for the set of target points. Note that the structural nodes associated with the displacement vectors are a subset of the nodes associated with the loadings.

Furthermore, assume that at a particular elevation angle γ, the surface is adjusted to compensate the gravity loading deflections. This angle is called the "rigging angle" and defines the elevation attitude at which the surface is ideally a perfect paraboloid. At any other elevation angle α, the net displacement is therefore:

$$\{u\} = \eta \{u_y\} + \zeta \{u_z\} \tag{7}$$

where, as can be seen from Fig. 2,

$$\left.\begin{aligned} \eta &= \cos\gamma - \cos\alpha \\ \zeta &= \sin\gamma - \sin\alpha \end{aligned}\right\} \tag{8}$$

In practice, it is appropriate to consider the pathlength differences with respect to an alternative paraboloid that best fits the data. The alternate paraboloid is defined by a maximum of six "homology" fitting parameters as follows:

H_x = vertex shift parallel to the X axis

H_y = vertex shift parallel to the Y axis

H_z = vertex shift parallel to the Z axis

θ_x = rotation about the X axis

θ_y = rotation about the Y axis

K = focal change parameter = (original focal length/new focal length) − 1

For structures and loading symmetric about the Y–Z plane, the parameters H_x and θ_y are zero. The focal change parameter K is justified if the antenna has a dynamically adjustable focal point.

The following additional terms are defined:

$\{\rho_y\}, \{\rho_z\}$ = half pathlength differences vectors from the best fitting paraboloid for the corresponding loadings.

SS_y = sums of squares of half pathlength differences for Y-loading = $\{\rho_y\}^t \{\rho_y\}$

SS_z = sums of squares of half pathlength differences for Z-loading = $\{\rho_z\}^t \{\rho_z\}$

$S_{yz} = \{\rho_y\}^t \{\rho_z\}$

The sum of the squares of the half pathlength differences SS_α from the best-fitting paraboloid at elevation angle α can be expressed as

$$\{p\}^t \{p\} = \eta^2 SS_y + \zeta^2 SS_z + 2\eta\zeta \{p_y\}^t \{p_z\} \tag{9}$$

or

$$SS_\alpha = \eta^2 SS_y + \zeta^2 SS_z + 2\eta\zeta S_{yz} \tag{10}$$

The rms half pathlength difference is

$$(\text{rms})_\alpha = (SS_\alpha/n)^{1/2} \tag{11}$$

where n is the number of points in the target set. In practice it is customary to incorporate weighting factors

in Eqs. (9) and (10) to represent the relative importance (such as the local tributary aperture area) of each of the points in the target set. For simplicity of presentation, it is assumed here that all points are of equal weight.

Here, during the design procedure, we will choose the rigging angle to make the pathlength differences at the horizon and zenith attitudes equal. Although there are other choices that are logical, this will result in the smallest peak rms difference over the entire elevation attitude range. Then a simple computation gives the rigging angle directly as follows:

$$\gamma = \phi - \varepsilon \tag{12}$$

where

$$\varepsilon = \tan^{-1}\left(\frac{B}{A}\right)$$

$$\phi = \cos^{-1}\left(\frac{C}{[A^2 + B^2]^{1/2}}\right) \tag{13}$$

and the terms A, B, C in Eq. (13) are

$$\left.\begin{aligned} A &= 2SS_y - 2S_{yz} \\ B &= 2SS_z - 2S_{yz} \\ C &= SS_y - SS_z \end{aligned}\right\} \tag{14}$$

Then, because the computation of rigging angle will produce equal rms values at horizon and zenith, either of these two attitudes presents a suitable design loading case for reducing the extreme rms variation over the entire elevation range. It also has been found that the rigging angle is reasonably insensitive to change with respect to alternative designs with moderate differences, which is helpful during iterative design because the rigging angle computed for a previous design is taken as the rigging angle for development of the following design.

Then, from the foregoing, the infinite spectrum of loading cases that result from the continuous range of elevation attitudes from horizon to zenith is effectively replaced by a single design loading case. Therefore for design the real loading could be formed as

$$\{P\} = \eta\,\{P_y\} + \zeta\,\{P_z\} \tag{15}$$

However, it is preferable to apply $\{P_y\}$ and $\{P_z\}$ separately to determine the associated displacement and half pathlength vectors. Following this, a typical load D_k of the dummy loading vector $\{D\}$ is computed to have the magnitude

$$D_k = \gamma_z \cdot (\eta\rho_y + \zeta\rho_z) \tag{16}$$

Equation (16) is evaluated at the kth target point and the load is applied normal to the surface at the point. Equation (16) follows from Eqs. (2) and (3) and the assumed linearity of displacements with respect to loading.

To use either the horizon or zenith attitudes as the design loading condition, α is set equal to 0 deg or 90 deg, respectively, in Eq. (8), and Eq. (7) is used in the computation of $\{S\}$ for Eq. (5). The displacements for the loading $\{D\}$ (Eq. 16) are used in the computation of $\{U\}$ for Eq. (5).

D. Design Algorithm

For design, we consider that the m bars of the structure are treated as a set of g bar groups, in which the ith group contains C_i bars of common area A_i. Consequently, the design variables become the group areas rather than the individual bar areas. There is no loss of generality in this, since a group can consist of $C_i = 1$ bar. The group length L_i is defined as the total length of bars in the group, or

$$L_i = \sum_{j=1}^{C_i} L_j \tag{17}$$

Also define a force term F_i for the ith group as

$$F_i = 1/L_i \sum_{j=1}^{C_i} S_j U_j L_j \tag{18}$$

Therefore, the virtual work W_i of the internal bar forces for the ith group is

$$W_i = (L_i F_i)/(A_i E) \tag{19}$$

For a structure comprising bars of the same material the constraint on total structure weight can be replaced by a volume constraint. Let V_p be the assigned volume of the bars; then the volume constraint is

$$\sum_{i=1}^{g} L_i A_i - V_p = 0 \tag{20}$$

Then, considering only the constraint of Eq. (20), we form the function G, which consists of the objective function augmented by the constraint equation times the Lagrange

multiplier λ. The objective function is formed by summing Eq. (19) over all the bar groups, thus

$$G = 1/E \sum_{i=1}^{g} (L_i F_i)/A_i + \lambda \left(\sum_{i=1}^{g} L_i A_i - V_p \right) \qquad (21)$$

Taking the partial derivative of G with respect to A_i and setting this equal to zero results in g equations that will ideally lead to the optimal values of the design variables. The equations are of the following type:

$$0 = -(L_i F_i)/(A_i^2 E) + \lambda L_i \qquad (22)$$

Solving Eq. (22) for each A_i, we obtain the new value

$$A_i = [F_i/(\lambda E)]^{1/2} \qquad i = 1, 2, 3, \cdots, g \qquad (23)$$

Using Eqs. (23) in Eq. (20), λ can be found from

$$(\lambda E)^{1/2} = 1/V_p \cdot \sum L_i \cdot F_i^{1/2} \qquad (24)$$

E. Restrictions and Modifications for Design Algorithm

Subject to restrictions that will be discussed subsequently, Eq. (23), in conjunction with Eq. (24), can be used to determine new values of the design variables A_i that will minimize the objective function for a constant weight of structural members. Nevertheless, the restrictions on the use of these equations are significant and require special modifications in the application.

The restrictions are:

(1) In differentiating Eq. (21), it was assumed that F_i is not a function of A_i. This is strictly true only in the case of statically determinant structures. The typical antenna structure contains a substantial number of redundant bars, so that the foregoing derivations are only approximately true.

(2) A side constraint could be violated by choosing A_i according to Eq. (23). Side constraints that are applicable are specific minimum areas to preclude stress or buckling failure. Another type of side constraint can be imposed to prevent unduly large changes with respect to the bar sizes of the preceding design. This will be called a "step-size ratio" limit and will be explained in conjunction with restriction 1.

(3) The ith group can be specified as a group for which no size changes are permitted.

(4) The F_i term for a particular group could be negative. Therefore, Eq. (23) becomes meaningless for real variables.

The first restriction entails an approximation in developing a new design. This approximation, plus the effects of bar grouping and variation of load distribution, are the only parts of the procedure that appear to be mathematically "inexact." The consequences are the requirement for an iterative design procedure in which the design approximations are corrected iteratively from cycle to cycle. Nevertheless, the magnitude of the approximations and corrections needed can be controlled to some extent by defining a limiting change in the design variables permitted from cycle to cycle. This step size ratio change R is employed to define the following restriction:

$$\text{abs}\,(\underline{A}_i - A_i)/A_i \leq R \qquad (25)$$

where $\underline{A}_i$ is determined from Eq. (23) and A_i is the design variable at the beginning of the cycle.

If the inequality is violated, the new design variable $\underline{\underline{A}}_i$ is established temporarily as follows:

$$\underline{\underline{A}}_i = A_i\,(1 + R\,\text{sgn}\,(\underline{A}_i - A_i)) \qquad (26)$$

The modification applied in conjunction with the second restriction is to test each $\underline{A}_i$ computed from Eq. (23) or $\underline{\underline{A}}_i$ computed from Eq. (26) against the specified minimum area and to select the most critical from the test. The modification for the third restriction is to exclude the group from redesign.

The fourth restriction is accounted for by a major change in the design algorithm. The groups are identified according to whether or not F_i is positive or negative. When positive, the group is treated as described above. When negative, objective and constraint are interchanged in the Lagrange multiplier formulation. Now the constraint becomes the internal virtual work for the positive groups and the objective is to minimize the volume of the negative groups. The constraint is taken to balance the positive virtual work as

$$SS_p - 1/E \cdot \sum (L_i \cdot F_i)/A_i = 0 \qquad (27)$$

In Eq. (27), the summation is taken over only the groups with negative F_i, and SS_p is the predicted objective function resulting from new sizes of the bars with positive F_i. It can be shown from Eqs. (23) and (24) that

$$SS_p = \lambda \cdot V_p \qquad (28)$$

Then by reformulating the Lagrange multiplier algorithm, we find for the bars with negative F_i

$$A_j = (-F_j)^{1/2} \cdot \sum_i [(-F_i)^{1/2} \cdot L_i]/(SS_p \cdot E) \qquad (29)$$

Ideally, Eq. (29) would provide a zero objective function and structure of smaller volume than specified. However, in practical applications, the first two restriction categories preclude the ideal situation.

It can be seen that all of the restrictions and modifications, except for the fourth, cause violations of the constant volume constraint. This is overcome in the execution of the design algorithms by a procedure that maintains the volume for each design and also develops the design closely in accordance with the foregoing theory.

Before applying the Lagrange multiplier algorithm to the design groups, their F terms and volumes are identified as "positive," "negative," or "excluded." Then, within each cycle, the first operation is to apply Eq. (23) to the positive groups. This can result in some of the groups being bounded from either above or below. Lower bounds are recognized, but upper bounds from this operation are ignored.

The positive volume is then adjusted by removing the volume of lower-bounded groups and adjusting the augmented objective function (Eq. 21) accordingly. The algorithm is re-applied, and as the result some groups will no longer be at their upper bounds and some new groups may become lower-bounded. Again, lower bounds are recognized, upper bounds ignored, and the procedure is repeated until no new lower bounds appear.

After this, Eq. (29) is applied exactly once to the negative groups. Since the result of this application will permit new volume to be assigned to the positive groups, the augmented objective function is reconstructed and Eq. (23) is applied one more time.

If any unbalanced volume remains after this, it is distributed by proportion to positive and negative groups in a manner that will not violate any of the constraint boundaries. Although this results in repeated applications of the design algorithms during each design cycle, the arithmetic is performed on one-dimensional vectors of size equal only to the numbers of design variables. Accordingly, execution of the design algorithms proceeds rapidly and expends only a relatively small proportion of the computation time for each cycle.

VI. Example Applications

A. Computer Program

A computer program has been developed to implement these procedures. In its current form, it is a prototype of a larger-capacity program that is intended to have design capability for antenna structures in the 64-m-diameter class or larger. At present, problem size is restricted to the in-core capacity of the Univac 1108, Exec 8 Computer. Nevertheless, as will be seen, reasonably sized demonstration problems can be processed.

The program logic is designed especially for the problem at hand and takes advantage of favorable related features wherever possible. This, in conjunction with the present in-core computational feature, results in rapid execution of numerous design iteration cycles. For example, the execution time to design the sample structures that will be described later has been compared with the execution time to perform a verification static load-deflection analysis of the same structures with both the NASTRAN and SAMIS structural analysis programs. The design program has been found to generate complete designs, executing about ten iteration cycles within the same or less time required by either of these two programs. The additional time required following both analysis programs for a post-processor to perform the rms pathlength difference computations is not included in this comparison.

The primary size restriction of the design program is the size of the structural stiffness/decomposition. This is stored as a rectangular matrix with the number of rows equal to the number of elastic degrees of freedom and the number of columns equal to the matrix bandwidth. A problem size of 260 degrees of freedom with a bandwidth of 75 can be designed using one 65K core bank. The program is devised to recognize externally developed nodal sequencing definitions to control the bandwidth. The bandwidth definition is used only for storage arrangement and not for the stiffness matrix decomposition algorithm. A conventional LDU algorithm is modified to avoid the computations associated with the empty terms within the band during matrix decomposition.

The program user establishes the step size ratio R and the maximum number of associated iterations permissible. If the design objective converges to within a 1% change before this number of iterations is reached, this sequence of iterations is terminated. The best design from this sequence is identified as the starting point for new sequences of iterations with reduced step sizes. At pro-

gram termination, properties of the best design attained are punched on cards for a restart or for execution on another program.

Much of the data input is in NASTRAN format and an existing NASTRAN data deck will require only a limited amount of additional preparation for the design program. However, the only type of element connections and properties recognized are the NASTRAN CBAR, PBAR, and CONROD definitions.

B. Sample Problems

1. Baseline structure. The hypothetical antenna structure shown in Fig. 3 was used as a basis for computer program development and evaluation. This is called the "baseline structure" and represents a highly simplified model of a practical reflector. It contains most of the essential features of typical reflector frameworks, but the surface and structure have been subdivided into a relatively coarse grid to expedite the computations.

There are six identical ribs spaced at 60-deg increments, which are interconnected by the customary hoop and diagonal members. Three supports are shown at nodes 201, 203, and 205. The plane of the supports is taken to be capable of rotation about the X-axis to vary the elevation attitude.

The Y–Z plane is a plane of symmetry. There are a total of 19 nodes, with three translational degrees of freedom permitted for each node. Therefore, excluding supports, there are 48 degrees of freedom in the model. Surface target nodes are 101, 301–306, 401–406, which provide 13 points for rms computation. There are six framing members of identical topology and similar structural function in each of ten different design groups (five rib-member, three hoop-member, two diagonal-member), resulting in a total of 60 members.

The design program started from an initial structure in which the design variables for all groups were the same. All groups throughout the procedure were constrained to minimum area equal to one quarter of the starting area. The external nonstructural weight is equal to about twice the weight of the structural members and is applied to simulate loading of nonstructural surface panels.

2. Validation structure. This is a second structure established for program evaluation and is patterned closely as a coarse-grid approximation to the analytical model of an existing 26-m-diameter antenna. The validation model contains about half as many radial ribs and circumferential hoop rings as the prototype. It also comprises members that simulate quadripod and counterweight structures and includes associated subreflector and ballast loads. The members of these components, since they are highly idealized, are placed in groups that are excluded from the design process. The typical inner "square girder" reflector support systems are also simulated.

Member sizes for the starting design were established to have cross section area distributions in similar proportion to the prototype. Minimum sizes were established to be approximately equal to one quarter of the initial. Because of symmetry with respect to the Y–Z plane, only one-half of the structure is considered. This half-section contains seven radial ribs and four rings, two legs of a quadripod, and the relevant portions of a counterweight and square girder. The structure is supported at the square girder by simulated elevation axis and ball-screw jack attachments.

The analytical model contains 83 nodes, 47 surface target points for rms computation, and 282 bars that are assigned to 56 design groups. Four groups are excluded so that 52 design variables are considered. There are 249 elastic degrees of freedom in the model, of which 26 are constrained, either by virtue of support or symmetry. The external nonstructural weight, which is predominated by the counterweight ballast simulation, is about three times that of the structural members. No sketch is included here to further describe the model.

VII. Results and Conclusions

Figure 4 shows the results of design iterations for the baseline structure. One sequence of 11 iterations with $R = 0.25$ is shown. The best rms value is obtained at cycle number 9, and the rms value here is about 55% of the initial. The horizon attitude loading was the design case, with rigging angle established to equate the zenith rms to the horizon rms. It can be seen here that the iterations proceed smoothly towards the best design.

The design for this problem was also run with larger values of R for initial sequences of five cycles followed by second sequences for which R was reduced. The results were considerably more erratic, but the effectiveness of the final designs thus obtained were about the same. In evaluating the design improvement shown, it should be noted that the objective is actually the sum of squares and not the rms values that are plotted. Therefore the final rms ratio of 55% is equivalent to a ratio of 30% on the mathematical design objective.

The iterative results obtained for the validation structure are shown on Fig. 5. Three iteration sequences are indicated in which up to four new designs per sequence were specified with $R = 0.60$, 0.24, and 0.12. The horizontal scales for the cycle numbers are in the approximate proportions of the related step size ratios.

As for the baseline structure, the horizon attitude was the design loading configuration. The rms value at the end of the fourth design of the first sequence was 46% of the starting value. The best design for the second sequence was found at its third cycle, equal to 36% of the initial. The third sequence achieved 32% of the initial rms value at the end of the third iteration and terminated here because of the convergence criterion (equivalent to ½% change on rms). The 1108 computer execution time for all of the 11 design iterations plus the starting design analyses to initiate each sequence was less than 2 min. Each iteration was executed in about 8 s, and much of this time was consumed in preparing a substantial amount of response data and information for output.

It can be seen, especially in Fig. 5, that relatively large step size ratios tend to produce erratic convergence; the convergence becomes smoother as the ratio decreases. Establishing effective ratios appears to be the key toward most efficient program usage. However, the results of many other sample design tests for these structures with different ratios and sequence specifications indicate that there is no consistently best way to approach all problems. This became evident for the baseline structure when the design grouping constraints were relaxed to permit up to 60 design variables. As expected, this relaxation produced further improvements of the objective. However, the most significant finding was that in some cases large ratios permitted large undesirable jumps in the convergence and, in other cases, the design appeared to alternate between two distinguishable configurations. Notwithstanding the undisciplined behavior, some of these problem formulations were as effective as some of the better-behaved tests with smaller ratios. When very small ratios were specified they led to extremely smooth convergence rates that were not always particularly effective because of the slow rate of descent.

Here we attribute this anomalous behavior to the iteration algorithm, as discussed previously with respect to the restrictions and corresponding modifications for design application. The consequences of this mathematically unsatisfactory convergence lie in the number of iteration cycles required to achieve an effective design. However, in a practical sense, the difficulty is overcome by the rapid rate at which the iterations are executed.

The effect of variation of the structural weight distribution does not seem to impose serious difficulties in obtaining the solution. This was established for the baseline structure by setting the bar density equal to zero to retain only the invariant nonstructural weight during the design. No substantial difference or improvement was observed in the convergence behavior.

It currently appears that the best way to approach a new design problem with no *a priori* knowledge of the convergence behavior is to establish a primary sequence with a large step size ratio and then reduce this successively. This provides the opportunity to find a point near a worthwhile minimum and to explore the region near this point more carefully in a subsequent sequence.

Present experience indicates that the reflector design problem (and possibly many other problems) is characterized by many local minima. It does not seem practical to explore all of these in an attempt to find the global optimum. A realistic appraisal of practical difficulties in structure design appears in Ref. 13. Nevertheless the program described here has been demonstrated to be an effective approach toward achieving a substantially improved design.

References

1. Schmit, L. A., "Problem Formulation, Methods and Solutions in the Optimum Design of Structures," *An Introduction to Structural Optimization*, Study No. 1, pp. 19–46, Solid Mechanics Division, University of Waterloo, Waterloo, Ontario, Canada, 1968.

2. Von Hoerner, S., "Homologous Deformations of Tiltable Telescopes," *J. Struct. Div., ASCE*, No. ST-5, Oct. 1967, pp. 461–485.

3. Chern, J. M., "Optimal Structural Design for Given Deflection in Presence of Body Forces," *Int. J. Solids Struct.*, 1971, Vol. 7, pp. 373–382, Pergamon Press.

4. Pierson, B. L., "A Survey of Optimal Structural Design Under Dynamic Constraints," *Int. J. Num. Meth. England*, Vol. 4, 1972, pp. 491–497.

5. Dupuis, G., "An Iterative Approach to Structural Optimization," *Int. J. Num. Meth. England*, Vol. 4, 1972, pp. 331–336.

6. Gellatly, R. A., Berke, L., and Gibson, G., "The Use of Optimality Criteria in Automated Structural Design," *Third Conference on Matrix Methods in Structural Mechanics*, Wright Patterson Air Force Base, Ohio, Oct. 19–21, 1971.

7. Venkaya, V. B., "Design of Optimum Structures," *Conference on Computer Oriented Analysis of Shell Structures*, Palo Alto, California, Aug. 10–14, 1970.

8. Kicher, T. P., "Optimum Design–Minimum Weight Versus Fully Stressed," *J. Struct. Div., ASCE*, Vol. 92, No. ST6, Dec. 1966, pp. 265–279.

9. Levy, R., "A Method for Selecting Antenna Rigging Angles to Improve Performance," in *The Deep Space Network*, Space Programs Summary 37-65, Vol. II, pp. 72–76, Jet Propulsion Laboratory, Pasadena, Calif., Sept. 1970.

10. Levy, R., "Antenna Rigging Angle Optimization Within Structural Member Size Design Optimization," in *The Deep Space Network Progress Report*, Technical Report 32-1526, Vol. I, pp. 81–87, Jet Propulsion Laboratory, Pasadena, Calif., Feb. 15, 1971.

11. Levy, R., and Melosh, R., "PARADES Structural Design System Capabilities," in this volume of *The Deep Space Network Progress Report*.

12. Utku, S., and Barondess, S. M., *Computation of Weighted Root-Mean-Square of Path Length Changes Caused by the Deformations and Imperfections of Rotational Paraboloidal Antennas*, Technical Memorandum 33-118, Jet Propulsion Laboratory, Pasadena, California, Mar. 1963.

13. Cornell, C. A., "Examples of Optimization In Structural Design," *An Introduction to Structural Optimization*, Study No. 1, pp. 143–164, Solid Mechanics Division, University of Waterloo, Waterloo, Ontario, Canada, 1968.

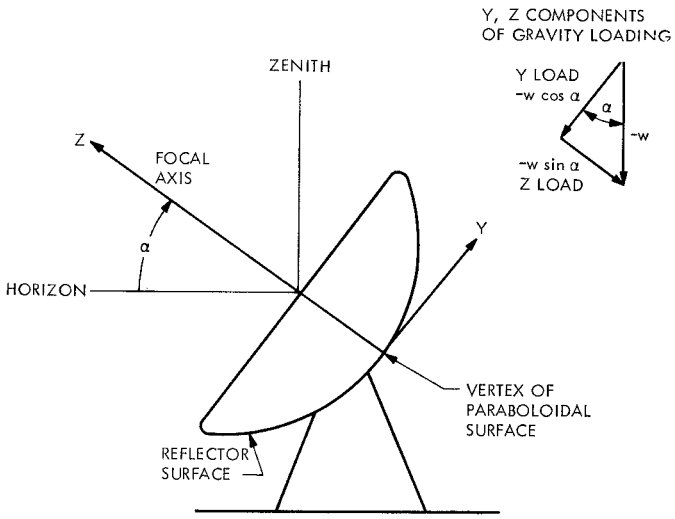

Fig. 1. Coordinate system for reflector

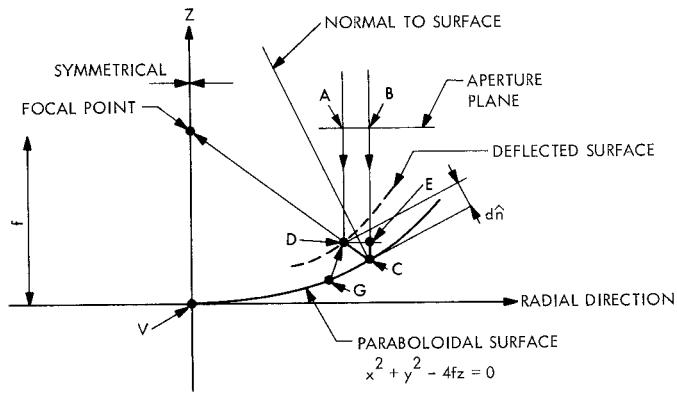

Fig. 2. Deflection geometry

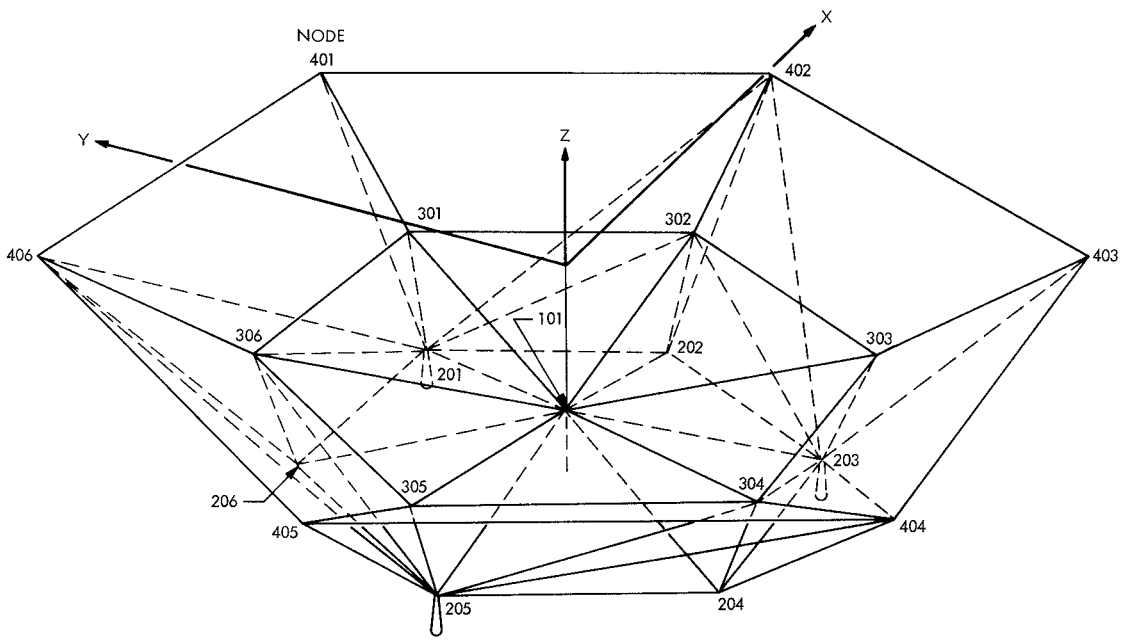

Fig. 3. Model of baseline structure

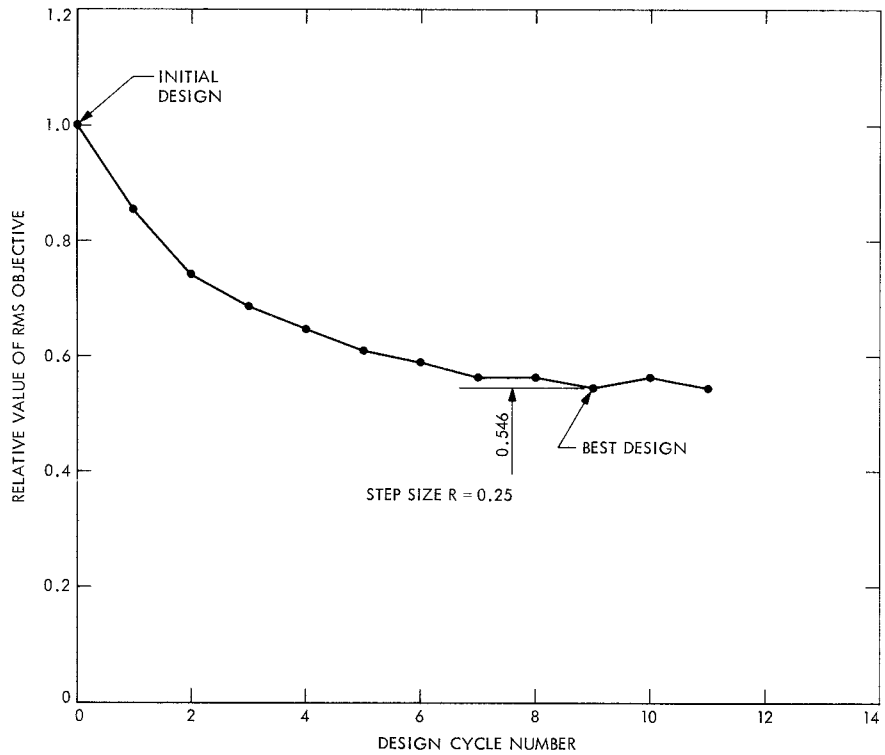

Fig. 4. Baseline structure design iterations

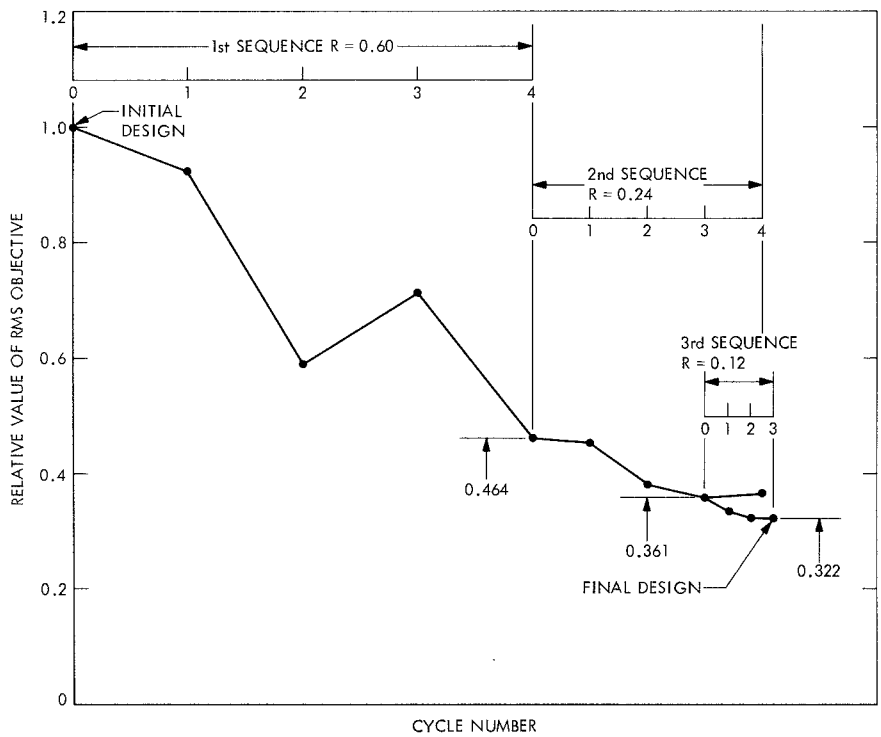

Fig. 5. Validation structure design iterations